Journal of Quantitative Spectroscopy & Radiative Transfer 110 (2009) 2115–2126

Contents lists available at ScienceDirect

Journal of Quantitative Spectroscopy & Radiative Transfer

journal homepage: www.elsevier.com/locate/jqsrt

Fourier transform measurements of SO_2 absorption cross sections: II. Temperature dependence in the 29 000–44 000 cm^{-1} (227–345 nm) region

A.C. Vandaele *, C. Hermans, S. Fally

Institut d'Aéronomie Spatiale de Belgique, 3 Av Circulaire, B-1180 Brussels, Belgium

ARTICLE INFO

Article history:
Received 2 February 2009
Received in revised form
8 May 2009
Accepted 12 May 2009

Keywords:
Laboratory measurement
Absorption cross section
Fourier transform spectroscopy
Sulfur dioxide

ABSTRACT

This paper is the second of a series that reports results on the measurements of the absorption cross section of SO_2 in the UV/visible region at high resolution and that investigates high temperatures in support to planetary applications. Absorption cross sections of SO_2 have been obtained in the 29 000–44 000 cm^{-1} spectral range (227–345 nm) with a Fourier transform spectrometer at a resolution of 2 cm^{-1} (0.4500 cm MOPD and boxcar apodisation). Pure SO_2 samples were used and measurements were performed at room temperature (298 K) as well as at 318, 338 and 358 K. Temperature effects in this spectral region are investigated and are favorably compared to existing studies in the literature. Comparison of the absorption cross section at room temperature shows good agreement in intensity with most of the literature data, but shows that most of the latter suffer from inaccurate wavelength scale definition. Moreover, literature data are often given only on restricted spectral intervals. Combined with the data described in the first part of this series of papers on SO_2, this new data set offers the considerable advantage of covering the large spectral interval extending from 24 000 to 44 000 cm^{-1} (227–420 nm), at the four temperatures investigated.

1. Introduction

This paper follows a previous paper [1] (referred as PI in the following), in which we reported the measurement of the absorption cross section of sulfur dioxide (SO_2) in the 24 000–29 000 cm^{-1} spectral region (354–420 nm) at room temperature (298 K) as well as at 318, 338, and 358 K. This second paper concerns the measurements of the absorption cross section of SO_2 in the 29 000–44 000 cm^{-1} spectral region (227–345 nm), which is normally used in atmospheric detection and observation of SO_2 in the Earth atmosphere [2–6], as well as in the atmosphere of other planets or celestial bodies [7–12].

SO_2 absorbs in three main regions in the near ultraviolet. The strongest band lies in the 45 000 cm^{-1} (220 nm) region and corresponds to the $\tilde{C}^1B_2 - X^1A_1$ electronic transition. Between 29 000 and 40 000 cm^{-1} extends a medium absorption structure, which can be ascribed to at least two electronic transitions. Underlying the structured bands of the A^1A_2–X^1A_1 [13], the 'continuous' absorption has been attributed to the B^1B_1–X^1A_1 transition [14,15]. The allowed transition B^1B_1–X^1A_1 is so perturbed that no rotational or vibrational analysis is possible. It forms a continuum due to the density of weak

* Corresponding author.
E-mail addresses: AnnC@oma.BE, a-c.vandaele@aeronomie.be (A.C. Vandaele).

0022-4073/$ - see front matter © 2009 Elsevier Ltd. All rights reserved.
doi:10.1016/j.jqsrt.2009.05.006

absorptions. The third weak absorption feature has been assigned to the a^3B_1–X^1A_1 electronic transition and was the subject of the previous paper.

This second paper which deals with the 29 000–44 000 cm^{-1} region, investigates the B^1B_1–X^1A_1 (perturbed by A^1A_2–X^1A_1) electronic transition, as well as the first absorption structures associated to the $\hat{C}^1B_2 - X^1A_1$. The aim of the present work is to provide absorption cross sections at a higher than previously reported resolution and to investigate high temperatures in support of planetary applications.

2. Experimental description

The experimental set up has been extensively described in the first part of the series and will be only briefly summarized here. Measurements of the absorption cross sections of gaseous SO_2 have been performed at the resolution of 2 cm^{-1} (maximum optical path difference = 0.4500 cm; 0.018 nm at 300 nm) over the 29 000–44 000 cm^{-1} (227–345 nm) spectral range under different pressure and temperature conditions with pure samples of SO_2. All measurements have been carried out with a Fourier transform spectrometer Bruker IFS120M in combination with either a Xenon high pressure lamp (150 W) or a Tungsten lamp (250 W), and with a GaP diode or a UV-Photomultiplier as detectors. The different combinations of lamp and detector allowed the recording of spectra in three different regions: (i) W-GaP: from 23 500 to 30 750 cm^{-1}, (ii) Xe-GaP: from 25 000 to 32 000 cm^{-1}, and (iii) Xe-PM: from 31 500 up to 45 000 cm^{-1}. The 200 cm long cell used during this study has already been described previously [1]. It can be temperature stabilized either by cooling it down by the circulation of a fluid around it, or by heating it by the use of a heating coil. Pressure was measured by 1000 and 10 Torr full scale temperature stabilized Baratron gauges.

SO_2 samples (Indugas, >99.98% stated purity) were used without further purification. One complete experiment at a given temperature consisted of: (i) a blank measurement (cell empty), (ii) measurement with the pure gas at several increasing and decreasing pressures, and finally (iii) a blank measurement. This procedure was repeated at least two times for each temperature. Spectra were recorded at 298, 318, 338, and 358 K in single-sided mode during the forward and backward movements of the mobile mirror. A boxcar apodization function was used. Depending on the experimental conditions, a certain number of mirror scans (interferograms) were averaged to get an acceptable signal to noise ratio. This number of scans was recorded in several blocks that were averaged at the end to obtain the spectrum. Recording successive blocks permitted following the pressure inside the cell, and was also used to monitor any change of absorption from one block to the other. The experimental conditions are summarized in Table 1. In the case of the Xe-PM combination, the number of scans per block was higher. Some experiments were carried out throughout the night enabling a large number of blocks to be obtained (see Table 1, numbers in brackets).

Table 1
Experimental description of the measurements used to obtain the SO_2 absorption cross sections at the different temperatures investigated in this study.

T (K)	Lamp-detector	Nb of different pressures	Pressure range (Torr)	Nb of co-added scans[a]	Duration of measurement (h)
298	W-GaP	10	31–130	40 × 128	1
	Xe-GaP	5	0.4–66.2	40 × 128	1
	Xe-PM	10	0.03–3.83	8 × 512	3
				(48 × 512)	(17)
318	W-GaP	11	31–150	40 × 128	1
	Xe-GaP	5	0.4–63.7	40 × 128	1
	Xe-PM	9	0.05–3.24	8 × 512	3
				(38 × 512)	(11.5)
338	W-GaP	14	20–175	40 × 128	1
	Xe-GaP	5	0.5–68.4	40 × 128	1
	Xe-PM	10	0.04–4.65	8 × 512	3
				(40 × 512)	(14)
358	W-GaP	15	30–265	40 × 128	1
	Xe-GaP	5	0.6–73.0	40 × 128	1
	Xe-PM	8	0.05–5.11	8 × 512	3
				(40 × 512)	(14)

For each lamp-detector combination and each temperature, the number of different SO_2 pressures and the range of pressures used are indicated. Each individual cross section is the result of the co-addition of several blocks made of 128 or 512 scans each. The duration of the measurements is also indicated. In some instance, measurements were performed for a whole night (between 11.5 and 17 consecutive hours). These correspond to the numbers in brackets.

[a] The total number of co-added scans is the results of the co-addition of all the scans performed in several successive blocks: 40 × 128 means that 40 blocks of spectra were recorded successively, and each of these blocks consisted of 128 scans of the moving mirror of the spectrometer.

3. Results

Absorption cross sections were obtained using:

$$\sigma(\nu) = \frac{1}{n_{SO_2} d} \ln\left(\frac{\frac{(I_{0,before}(\nu) + I_{0,after}(\nu))}{2}}{I(\nu)}\right) \quad (1)$$

where n_{SO_2} is the concentration of SO_2 inside the cell, d is the cell length, $I_{0,before}$ and $I_{0,after}$ are, respectively, the blank spectra recorded before and after the SO_2 measurement, and I is the intensity measured when the cell contained SO_2.

Fig. 1 shows the absorption cross section of SO_2 obtained at room temperature. As already discussed in PI, the final cross section is the average of all available individual cross section obtained under different pressure conditions. By varying the SO_2 pressure, different optical densities could be achieved, allowing the best possible recording of absorption cross section along the entire spectral interval. For example due to the high cross section values around 34 000 cm^{-1}, recording was optimized in this region by using low concentrations of SO_2, leading to a very low signal to noise below 31 000 cm^{-1} and above 38 000 cm^{-1}. However, recording conditions optimized for the 29 000–30 000 cm^{-1} (high concentrations of SO_2) corresponded to spectra saturated in the 33 000–37 000 cm^{-1} region. Each individual spectrum was therefore only used on a restricted optimized spectral interval. These intervals were found as the best compromise between enough signal and no saturation. As an illustration, the intervals in the case of the Xe-PM spectra at room temperature are presented in Table 2. Fig. 2 illustrates the number of individual cross sections averaged as a function of wavenumber and for the different temperatures investigated. In general, the number of different spectra below 30 000 cm^{-1} is large because this region is

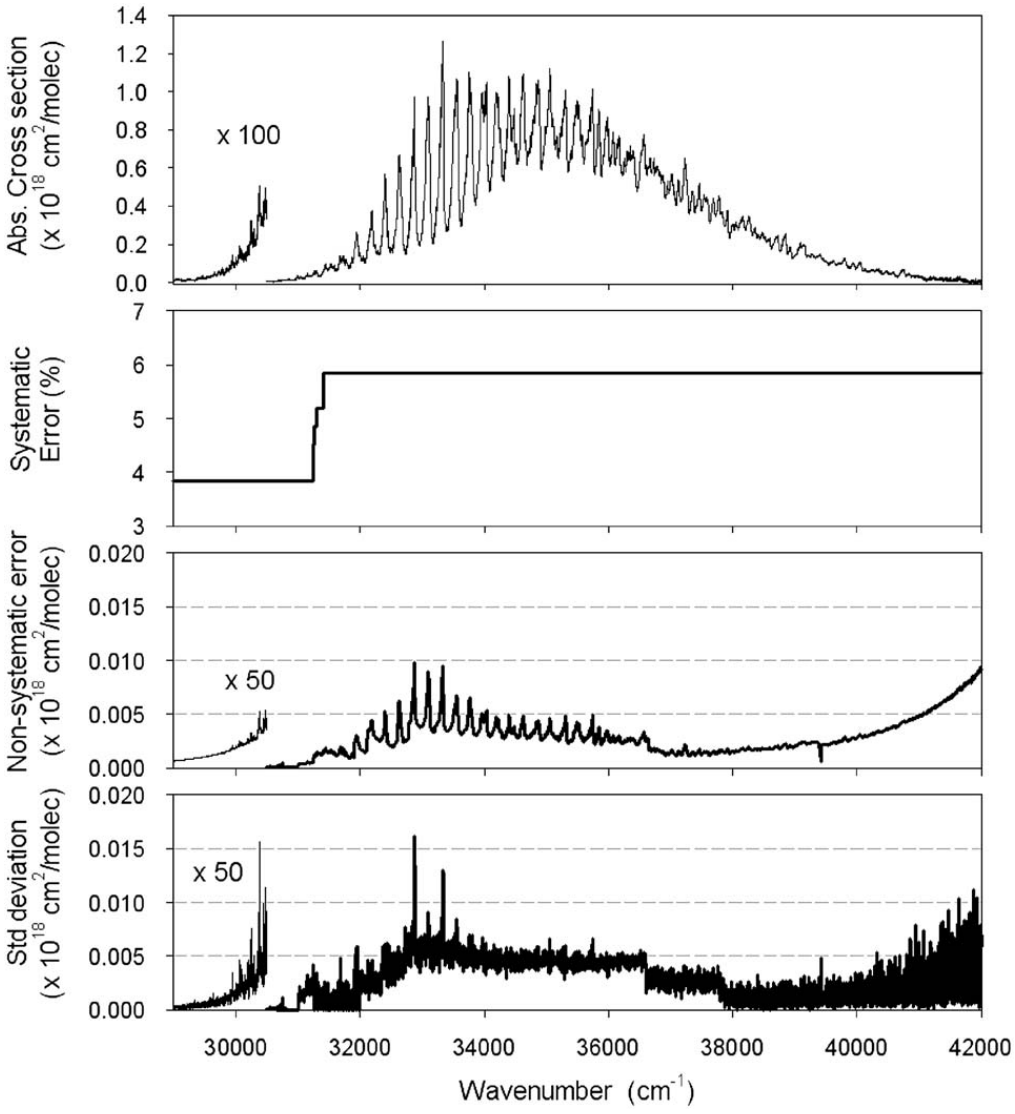

Fig. 1. Absorption cross sections of SO_2 at 298 K. The systematic and non-systematic errors are shown, as well as the standard deviations of the measurements, which represents their repeatability.

Table 2
Spectral interval on which each of the spectra obtained at room temperature using the Xe-PM combination is considered.

Case	SO_2 pressure (Torr)	Valid spectral interval (cm^{-1})
1	0.05	32 780–36 650
2	0.10	32 700–36 500
3	0.15	32 600–36 500
4	0.20	32 350–37 800
5	0.20	32 120–36 600
6	0.26	32 100–44 500
7	0.49	31 900–44 500
8	0.76	32 000–33 200+35 200–44 500
9	1.03	31 250–32 820+37 000–44 500
10	3.83	31 300–31 900+39 400–43 200

Pressures of SO_2 are also indicated. The final cross section at room temperature is the average of all these spectra considered only on their restricted spectral intervals.

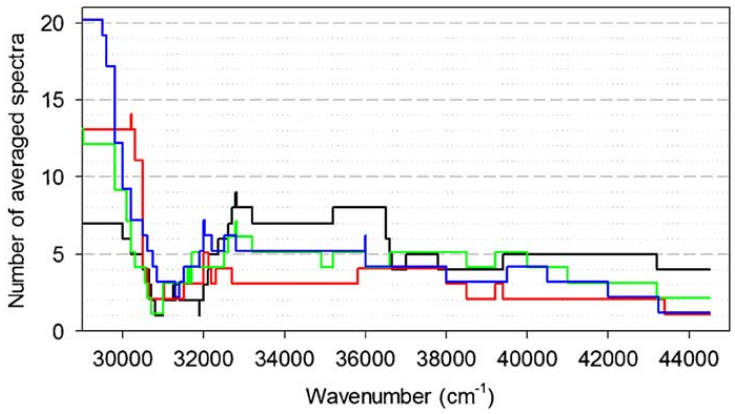

Fig. 2. Number of individual absorption cross sections which were averaged to obtain the final cross section at the different temperatures: (black) 298 K, (red) 318 K, (green) 338 K, and (blue) 358 K. (For interpretation of the references to color in this figure legend, the reader is referred to the web version of this article.)

covered by two lamp-detector configurations (W- and Xe-GaP). The worst area is between 31 000 and 32 000 cm^{-1} where it is difficult to obtain highly accurate spectra because of higher noise levels (Xenon lamp) and saturation limitations.

A way to check the quality of the measurements is to look at their repeatability through the determination of the standard deviation of the individual cross sections obtained at a given temperature with respect to their average. The standard deviation of all the measurements performed at room temperature is of the order of 0.005×10^{-18} cm^2/molec or less between 29 000 and 41 000 cm^{-1} (see Fig. 1, bottom panel). It is higher above 41 000 cm^{-1} where the signal to noise is poor. It also reaches higher values on some peak structures around 33 000 cm^{-1}. The standard deviation of the measurements reaches 0.015×10^{-18} cm^2/molec at the higher temperatures. These numbers are of the same order of amplitude as the systematic and non-systematic errors on the measurements, which are shown in the two middle panels of Fig. 1.

The uncertainties of the absorption cross sections have been estimated by considering different error sources: on the concentration, taking into account the uncertainties on the temperature (2 K, including the reading error, stabilization in time and along the cell) and the pressure (3%, reading and correction for the thermal transpiration [16]); and on the length of the cell (0.25%). Taking into account all these error sources, the total systematic uncertainty on the cross section has been estimated to be of the order of 4% below 31 500 cm^{-1} and 6% above from a simple error propagation calculation (see Fig. 1).

Non-systematic uncertainties on the absorption cross sections were also estimated. Those are mostly due to the noise level on the absorbance (i.e. the noise levels on I and I_0) and to the lamp drifts with time. Noise levels were evaluated as the rms standard deviation of the measured spectra where no absorption features are located. Lamp drift was estimated by looking at the evolution of the intensity of the lamp spectra recorded with the empty cell. This assumes that the evolution of the lamp spectrum in time does not vary with wavenumbers. It was found that the intensity variation was of the order of 1% for the W lamp and 3% for the Xe lamp over the duration of a complete measurement sequence (about 10 h). The uncertainties of the measurements performed at the higher temperatures are somewhat better because, as stated in Table 1, the number of different spectra is larger. In the case of the measurements at 358 K, up to 20 individual cross sections have been averaged. Systematic and non-systematic errors are also given in the files which are available from the website of the Belgian Institute for Space Aeronomy (http://www.aeronomie.be/spectrolab/).

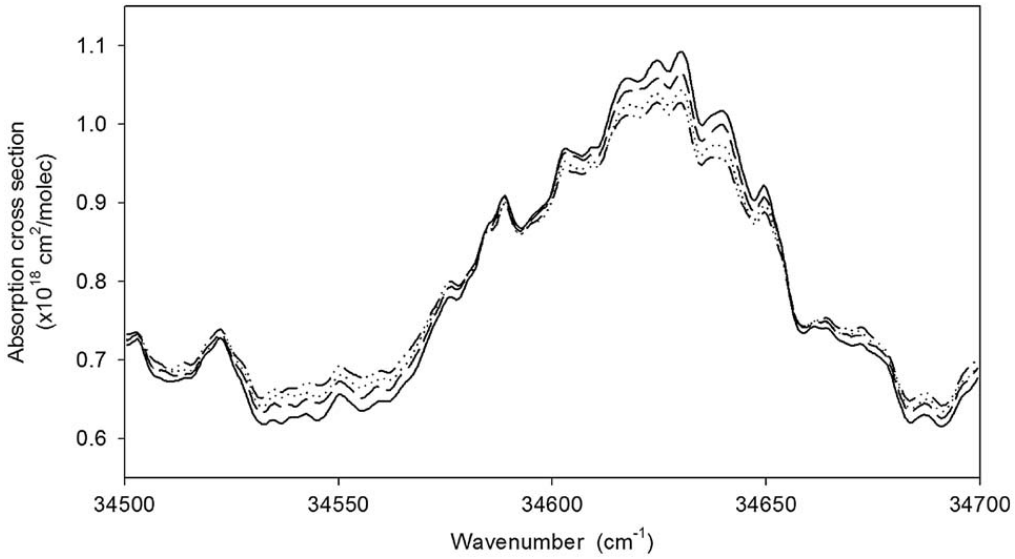

Fig. 3. Evolution of the SO_2 absorption cross section with temperature: (—) 298 K, (– – –) 318 K, (●●●) 338 K, and (–●●–) 358 K.

The wavenumber calibration has been performed using 37 lines of I_2, whose positions were taken from the Iodine atlas of Gerstenkorn and Luc [17,18]. Spectra of I_2 were recorded at the resolution of 0.042 cm^{-1} with the same instrument that was used for the measurements of SO_2. The wavenumber accuracy is estimated to 0.02 cm^{-1}, which represents the average value of the differences observed between the positions obtained in this work and those of the atlas. Note that the line positions of the atlas are given in vacuum and were first transformed to air wavenumbers using the Edlen formula [19], as the spectrometer was not operated under vacuum. Therefore, all wavenumbers given in this work are expressed in air and are defined as $1/\lambda_{air}$.

3.1. Temperature effect

The temperature effect was investigated by measuring the absorption cross sections at different temperatures (298, 318, 338, and 358 K). Fig. 3 illustrates the temperature effect on the absorption cross section: Intensities increase with temperature in the troughs and decrease with temperature near the peaks.

A linear temperature coefficient $c(\nu)$ is defined as

$$\sigma_T(\nu) = \sigma_{298\,K}(\nu) + c(\nu)(T - 298) \tag{2}$$

The choice of this simple description has already been discussed in PI. The $c(\nu)$ coefficient was obtained by least square fitting the absorption cross sections at the different temperatures and at a given wavenumber ν with the expression in Eq. (2), taking into account the experimental error on the measured values. The evolution of the temperature parameter is shown in Fig. 4 for a small spectral interval. The correlation coefficient of the linear regression is also plotted in this figure: it is equal to 1 at the peaks and −1 in between, with a very rapid transition from one value to the other, indicating the high linearity of the temperature effect. There is no clear and easy theoretical explanation for the observed temperature effect, as the absorption in the investigated region is due to two superposed transitions.

4. Comparison with data from the literature

SO_2 absorption cross sections have already been extensively investigated in the 30 000–40 000 cm^{-1} region at room temperature [20–34]. The temperature dependence was mainly investigated by looking at temperatures lower than room temperature [29,30,33]. Only a couple of measurements have been performed at higher temperatures [23,24]. Recently, Danielache et al. [35] investigated the effect of the isotopes of S on the absorption cross section of SO_2. Their measurements were performed at very low resolution (25 cm^{-1}) and were therefore not considered in our comparison exercise. Table 3 summarizes the experimental conditions of the existing literature data.

As explained in detail in PI, two major problems arise when comparing two data sets: (i) how to take accurately into account the different resolutions; (ii) how to calibrate the wavelength scales of the literature data. In general, a shift as well as a stretching of the scale should be introduced. In this study we have, however, limited the correction of the wavelength scale of the different literature data sets to a shift, as the introduction of a stretch would not change the conclusions of the comparison. In order to perform reliable comparisons between absorption cross-sections obtained at different resolutions, the data of the present work have been convolved with a Gaussian instrumental line shape (ILS) to correspond to the resolution of the literature data, which are reported in Table 3. Only the Rufus et al. data set [27] was obtained at a higher

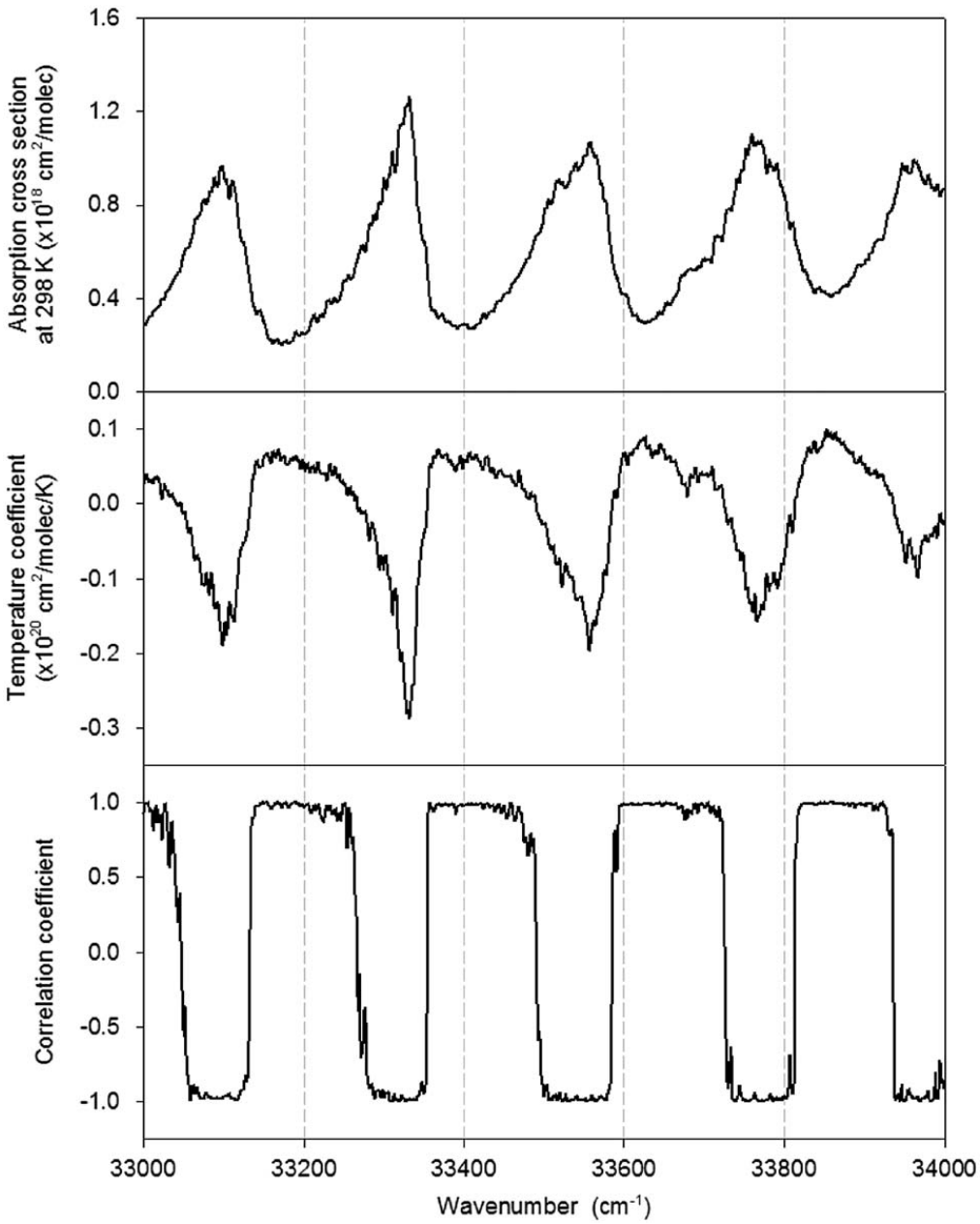

Fig. 4. Temperature dependence: (a) absorption cross section at 298 K, (b) temperature coefficient, and (c) correlation coefficient of the linear regression.

resolution than ours and these data have been convolved to correspond to the resolution used in the present work (using in this case the exact since ILS function of the FTS corresponding to a MOPD of 0.45 cm).

4.1. Room temperature

Results of the systematic comparison between the literature data and the data from the present study are summarized in Table 4. Each data set from the literature has been fitted by the linear expressions

$$\sigma_{Lit}(\lambda + shift) = a + b \times \sigma_{this\ work}(\lambda + convolution) \quad (3)$$

where the parameters a and b represent the offset and a multiplicative factor. For comparison purposes the shifts have also been converted into nanometers (conversion performed at the center of the spectral interval considered) and have to be compared to the announced accuracy on the wavelength scales of the literature data. We have also considered the possibility that the discrepancies observed between two data sets could be explained by using only a multiplicative factor, thus without any offset in intensity. This multiplicative factor is also given in Table 4 (parameter c). The comparison has been done for different spectral intervals: (1) on a largest possible interval limited by the common coverage of the two data sets compared and (2) on 2000 cm^{-1} wide intervals starting from 30 000 cm^{-1} to better investigate the evolution of the

Table 3
Description of existing literature data.

Author	T (K)	Region	Technique[a]	Resolution	Sampling	ε_{wn} (nm)	ε_{xs} (%)	Comment
Warneck et al. [20]	295	185–315 nm	H+G	0.1 nm	n[b]	n[b]	n[b]	
Thompson et al. [26]	295	296–302 nm	L	0.02 nm	0.01 nm	0.01	2	
Woods et al. [22]	293	297–301 nm	LD	0.002 nm	0.01 nm	0.002	6	
Brassington [32]	292–300	290–317 nm	L+LD	0.05 nm	0.02 nm	0.01	3	Average of several spectra taken at T ranging from 292 to 300
Wu and Judge [25]	294	299–339 nm	S+G	0.06 nm		0.05	10	
Leroy et al. [30]	218, 263, 292, 296	281–312 nm	D+G	0.2 nm (0.015 nm at 292 K)	1.4 nm	n[b]	4	
McGee and Burris [29]	210, 295	300–320 nm	D+G	0.03 nm	0.03 nm	0.01	2–10	
Hearn and Joens [31]	300	228–339 nm	D/W+G	0.06 nm	0.02 nm	0.03	4	
Vandaele et al. [21]	295	27 000–4000 cm^{-1} (250–370 nm)	X+FT	2 and 16 cm^{-1}	0.96 cm^{-1}		2.5	
Ahmed and Kumar [34]	300	279–320 nm	A+G	0.2 nm	0.17 nm	0.03	3	
Manatt and Lane [28]	293	106–403 nm	–	0.1 nm	0.1 nm	n[b]	n[b]	Compilation of literature data
Vattulainen et al. [23]	293, 873, 1073	195–350 nm	D+G+PM	0.5 nm	0.5 nm	0.1 nm	3	
Wu et al. [24]	200, 295, 400	208–295 nm	S+G	0.05 nm	0.005	0.05 nm	10	
Bogumil et al. [33]	203, 223, 243, 273, 293	230–395 nm	X/W+G	0.24 and 0.26 nm	0.12 nm	0.01 nm	3	Values at 293 K scaled to Vandaele et al.; others: surface indep. of T
Rufus et al. [27]	295	220–325 nm	X+FT	4–16 m Å	0.0006 nm	10 m Å	5	
Danielache et al. [35]	293	30 300–52 500 cm^{-1} (330–190 nm)	D+FT	25 cm^{-1}	8 cm^{-1}	n[b]	1.2	Isotopic effect

For each reference, the following information is given: temperature, spectral region, technique used, spectral resolution, uncertainty ε on the wavelength scale and on the cross section, and some general comment.

[a] A = Argon arc lamp; H = H_g lamp; D = Deuterium lamp; S = Synchrotron radiation; X = Xenon arc lamp; W = Tungsten lamp; G = grating; FT = Fourier transform spectrometer; L = dye laser; LD = dual beam dye laser; and PM = photomultiplier.

[b] n = Not specified.

Table 4
Results of the comparison of the SO_2 absorption cross sections at room temperature with data from the literature.

Reference	$\sigma_{Lit} = a+b \times \sigma_{This\ work}$		$\sigma_{Lit} = c \times \sigma_{This\ work}$	Shift	
	a (cm^2/molec)	b	c	(cm^{-1})	(nm)
Thompson et al. [26]					
[33 182–33 761]	1.80e−020	1.04	1.07	−0.2	−0.00
Brassington [32]					
[31 554–34 468]	8.24e−021	1.04	1.05	1.0	0.01
[31 554–32 000]	3.94e−021	1.03	1.06	−3.1	−0.03
[32 000–34 000]	1.02e−020	1.04	1.05	0.6	0.01
[34 000–34 468]	4.20e−021	1.04	1.04	4.3	0.04
McGee and Burris [29]					
[31 211–33 333]	2.11e−020	0.96	1.01	1.9	0.02
[31 211–32 000]	1.03e−020	1.00	1.09	−2.4	−0.02
[32 000–33 333]	3.20e−020	0.94	1.00	2.0	0.02
Hearn and Joens [31]					
[29 427–43 987]	3.36e−020	0.96	1.01	−1.4	−0.01
[30 000–32 000]	1.59e−021	1.07	1.08	−2.3	−0.02
[32 000–34 000]	3.04e−020	0.93	0.98	−1.2	−0.01
[34 000–36 000]	6.09e−020	0.92	0.99	−1.3	−0.01
[36 000–38 000]	8.37e−020	0.90	1.05	−3.2	−0.02
[38 000–40 000]	6.82e−020	0.97	1.28	−6.7	−0.04
[40 000–42 000]	4.43e−020	1.17	2.04	−11.6	−0.07
[42 000–43 987]	4.10e−020	1.13	1.41	−14.9	−0.08

Table 4 (*continued*)

Reference	$\sigma_{Lit} = a+b \times \sigma_{This\ work}$		$\sigma_{Lit} = c \times \sigma_{This\ work}$	Shift	
	a (cm^2/molec)	b	c	(cm^{-1})	(nm)
Vandaele et al. [21]					
[30 509–38 511]	1.43e−020	0.98	1.00	−0.4	−0.00
[30 509–32 000]	2.69e−021	1.01	1.04	−0.4	−0.00
[32 000–34 000]	1.34e−020	0.96	0.99	−0.4	−0.00
[34 000–36 000]	2.99e−020	0.96	0.99	−0.4	−0.00
[36 000–38 000]	4.00e−020	0.95	1.02	−0.5	−0.00
[38 000–38 511]	5.28e−020	0.92	1.11	−0.5	−0.00
Manatt and Lane [28]					
[29 000–44 000]	1.25e−020	1.03	1.05	1.5	0.01
[30 000–32 000]	2.03e−021	1.07	1.09	−5.9	−0.06
[32 000–34 000]	4.43e−020	0.96	1.03	1.8	0.02
[34 000–36 000]	2.37e−019	0.76	1.05	−3.6	−0.03
[36 000–38 000]	−1.72e−021	1.06	1.06	−20.9	−0.15
[38 000–40 000]	3.41e−020	0.94	1.09	−2.0	−0.01
[40 000–42 000]	1.69e−020	0.88	1.19	−30.6	−0.18
[42 000–44 000]	−2.75e−022	1.85	0.90	23.5	0.13
Vattulainen et al. [23]					
[29 025–44 000]	7.10e−020	1.00	1.12	−44.0	−0.32
[30 000–32 000]	2.11e−020	1.10	1.32	−32.3	−0.33
[32 000–34 000]	7.49e−020	0.96	1.10	−37.0	−0.34
[34 000–36 000]	2.82e−019	0.74	1.10	−30.7	−0.25
[36 000–38 000]	6.23e−020	1.02	1.13	−50.0	−0.37
[38 000–40 000]	7.92e−020	0.94	1.31	−40.2	−0.26
[40 000–42 000]	1.29e−019	0.18	2.84	−40.7	−0.24
[42 000–44 000]	1.80e−019	1.74	3.24	−9.3	−0.05
Wu et al. [24]					
[34 511–44 000]	3.11e−020	0.88	0.93	−15.0	−0.10
[34 511–36 000]	8.43e−020	0.82	0.92	−14.8	−0.12
[36 000–38 000]	4.91e−020	0.84	0.93	−15.3	−0.11
[38 000–40 000]	2.74e−020	0.91	1.03	−11.5	−0.08
[40 000–42 000]	2.81e−020	0.88	1.44	−9.7	−0.06
[42 000–44 000]	2.80e−020	0.96	1.15	−18.1	−0.10
Bogumil et al. [33]					
[29 000–41 850]	1.11e−020	0.99	1.00	−10.7	−0.09
[30 000–32 000]	4.46e−022	1.03	1.04	−9.7	−0.10
[32 000–34 000]	1.45e−020	0.98	1.01	−10.8	−0.10
[34 000–36 000]	4.35e−020	0.94	0.99	−10.5	−0.09
[36 000–38 000]	1.99e−020	0.98	1.01	−10.9	−0.08
[38 000–40 000]	2.84e−020	0.94	1.08	−8.5	−0.06
[40 000–41 850]	3.20e−020	0.88	1.55	−8.4	−0.05
Rufus et al. [27]					
[30 759–44 000]	6.36e−021	0.92	0.93	0.0	0.00
[30 759–32 000]	1.67e−021	0.90	0.92	0.0	0.00
[32 000–34 000]	3.47e−021	0.92	0.93	0.1	0.00
[34 000–36 000]	−5.02e−021	0.94	0.93	0.0	0.00
[36 000–38 000]	−1.04e−020	0.95	0.93	0.0	0.00
[3 8000–40 000]	2.11e−020	0.87	0.97	0.0	0.00
[40 000–42 000]	1.63e−020	0.92	1.19	0.3	0.00
[42 000–44 000]	1.86e−020	0.69	0.81	0.0	0.00

a represents the multiplicative factor existing between the values of this work and the literature data. The last column indicates the spectral shift $\nu_{Lit}-\nu_{This\ work}$, expressed in wavenumber and wavelength (conversion at the center of the interval).

shift and of the a and b parameters with wavenumber. The detailed comparison of the data obtained in this work with data from the literature is illustrated in Fig. 5, where the absolute differences are shown in the lower panels. In those comparisons, shifts (corresponding to the largest interval, see Table 4) have already been applied so that conclusions on the amplitudes of the cross sections can be drawn. It should be remembered that the choice of a Gaussian function as representative of a grating instrument is not perfect: it is only a good approximation to the exact instrument line shape. Moreover, the resolution (width of the ILS) is not necessarily constant on the entire spectral range investigated. This might explain some of the differences observed between two data sets, essentially around the peaks of absorption. Similar spikes are also introduced when there is a slight shift between the two spectral scales.

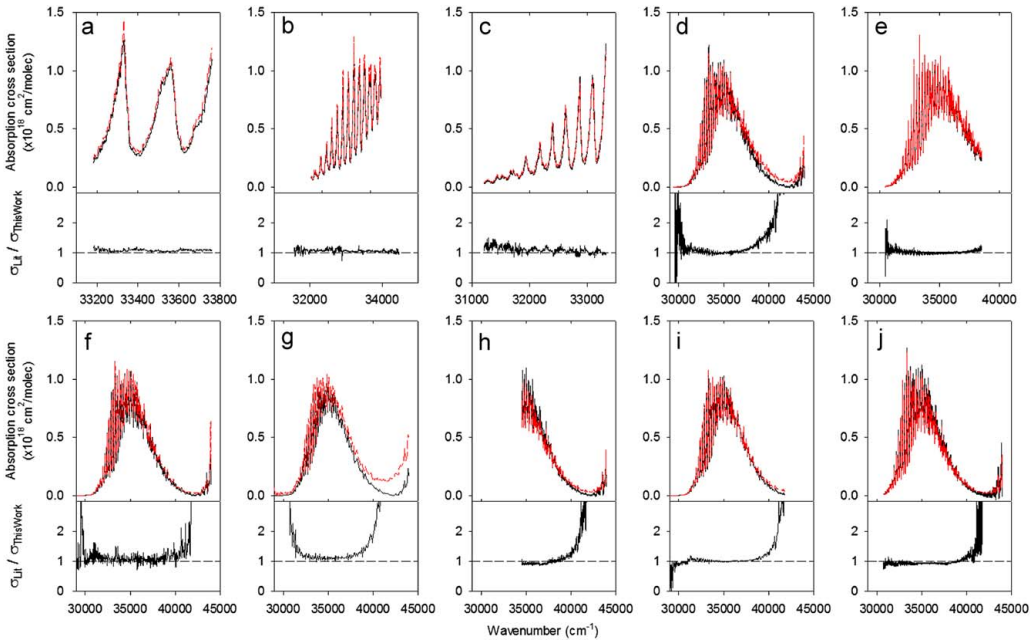

Fig. 5. Comparison of the SO_2 absorption cross section at 298 K of this work (black solid line) with data from the literature (red dash line): (a) Thompson et al. [26], (b) Brassington [32], (c) McGee and Burris [29], (d) Hearn and Joens [31], (e) Vandaele et al. [21], (f) Manatt and Lane [28], (g) Vattulainen et al. [23], (h) Wu et al. [24], (i) Bogumil et al. [33], and (j) Rufus et al. [27]. The bottom panels show the $\sigma_{Lit}/\sigma_{This\ work}$ ratios, the line representing unity. Data from the literature have been spectrally shifted in accordance to Table 4. (For interpretation of the references to color in this figure legend, the reader is referred to the web version of this article.)

Thompson et al. [26] investigated the 296–301 nm region using a frequency-doubled dye laser, which gave a very accurate wavelength scale. Indeed, the comparison with our new data shows that the shift between the two data sets is about 0.002 nm, which is far less than the announced accuracy (0.01 nm, see Table 3). Their cross section values are on average 7% larger than ours. Brassington's data [32] agree within 5% with the new data of this work. However, a wavelength shift exists which varies a lot on the common spectral interval and is larger than the stated accuracy. Data from McGee and Burris [29] are in very good agreement with our new data (within 1%), when considering the whole common spectral interval with a constant shift of about 0.02 nm, i.e. twice the accuracy on their wavelength values. However, below 32 000 cm^{-1}, the discrepancy is mainly due to an offset: if a small offset of 1.03×10^{-20} cm^2/molec is introduced, the agreement is nearly perfect. From Fig. 5(d), it can be seen that the cross section values from Hearn and Joens [31] are in good agreement with the new data (within 5%) between 32 000 and 38 000 cm^{-1} and are higher above, the discrepancy being explained by a mix of an offset and a multiplicative factor. There is also a wavelength shift growing from 0.01 to 0.08 nm but it is always lower than, or of the order of, the announced accuracy below 40 000 cm^{-1}. Comparison with the data of Vandaele et al. [21] shows an agreement of 2% between the two data sets over the 32 000–38 000 cm^{-1} range. They are higher outside those limits. Data of Vandaele [21], which have been obtained at the same resolution as that used in this work, and with a similar instrument, are, however, noisier because they result from the co-addition of a smaller number of individual spectra. A small wavenumber shift has been found. Note that these data were not calibrated with respect to well known absorption lines, such as in the present work. The data of Manatt and Lane [28] show variable agreement with the new data as a function of the spectral interval, which can be explained by the fact that they are a compilation from different literature sources. The good agreement observed for the largest interval and reported in Table 4 is, in our opinion, fortuitous, as large errors seem to compensate themselves over the wide interval. However, the values of the a and b parameters vary a lot from one small interval to the other. Note that the scale of the graph representing the Manatt's data (and also that of the Vattulainen's data) is different than that of the other plots. Vattulainen et al. [23] report values of the SO_2 absorption cross sections at 293 K at a resolution of 0.5 nm. The comparison also shows different agreement depending on the spectral interval considered. There is a practically constant wavelength shift of 0.3 nm lower than the estimated accuracy of 0.5 nm. Data of Wu et al. [24] are systematically lower than ours below 38 000 cm^{-1} and higher above (see Fig. 5(h)) and present a quasi-constant wavelength shift of 0.1 nm on the whole interval. Bogumil et al. [33] measured the SO_2 cross section at low resolution (0.24 nm) in support of the SCIAMACHY instrument on board the European ENVISAT-1 satellite. The overall agreement is better than 1% for the cross section intensities. There is a wavelength shift of 0.1 nm between the two data sets. Finally, the data of this work have been compared to those of Rufus et al. [27], who measured the absorption cross section of SO_2 at very high resolution (4–16 m Å). The comparison with our data was done after convolving their data to correspond to our resolution. The agreement on the intensity values is within 7% on average, the larger differences appearing at the peak, where, as already explained, some problems of convolution might be more critical. No wavenumber shift was detected between the two data sets, confirming the high accuracy of the wavenumber scales of both studies.

One can summarize on the basis of Table 4 and Fig. 5 that the present cross sections best agree with the data of Bogumil et al. [33] and of Vandaele et al. [21] wavenumber calibration problems aside. But, compared to the present work, previous Vandaele's data appear noisier, and Bogumil's optical densities at 293 K were scaled to the measurements of Vandaele et al. [26] and also cover a narrower spectral interval. Rufus' data [27] are also very interesting to compare with, because of their high resolution, but peak intensities are lower.

4.2. Higher temperatures and temperature effect

No measurement of the SO_2 absorption cross section could be found in the literature corresponding to the exact higher temperatures investigated in this study. We have thus based the comparison on the temperature effect, using only data sets with at least three different temperature measurements [24,33]. The comparison is illustrated in Fig. 6, for some selected wavenumbers, all comprised 36 000 and 38 000 cm^{-1}. This interval has been chosen because all three sets included in this comparison have data in this region. Data of this work and of Wu et al. have been convolved to the resolution of Bogumil et al. data, which have been obtained at the lowest resolution (0.24 nm). In this figure, data from Bogumil et al. [33] have been shifted by 10.7 cm^{-1} (see Table 4). Unexpectedly, the data of Wu et al. [24] presented different wavelength shifts for the different temperatures: data at room temperature were shifted by 15.0 cm^{-1} (see Table 4), those at 200 K by 10.0 cm^{-1}, and those at 400 K by 20.0 cm^{-1}. The existence of shifts due to the temperature has never been reported elsewhere and is not observed in the present work. Recently, Danielache et al. [35] reported shifts of the SO_2 absorption cross sections, but these were related to isotopic shifts which are expected by theory. To concentrate on the comparison of the temperature effect, intensities from Bogumil et al. and of Wu et al. were shifted so that values at room temperature were equal to the values found in this work. In that way, we eliminate the differences existing between the first term of the right-hand side of Eq. (2), $\sigma_{298\,K}(\nu)$, leaving only the comparison of the second term, the temperature effect. It is worth mentioning that the examples shown in Fig. 6 are all 'good' cases. In general, we have observed that: (i) the cross section values of Bogumil et al. at 273 K did not always follow the same evolution as the other Bogumil values. This was already discussed by Bogumil et al.: they attributed the different behavior to a lamp drift problem; (ii) the lowest temperature values from Bogumil et al. depart from linearity; and (iii) Wu et al. data showed little linearity. However, several approximations had to be introduced

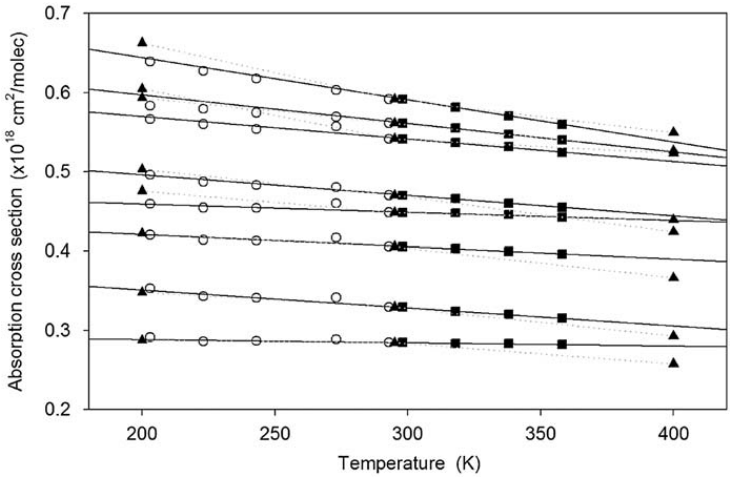

Fig. 6. Comparison of the temperature dependence of the SO_2 absorption cross section obtained in this study with temperature dependences from the literature: (■) this study, (○) from Bogumil et al. [33], and (▲ and dotted lines) from Wu et al. [24]. Solid lines represent the linear regression passing through the data of this work. To compare more easily the temperature effect, values obtained at room temperature of Bogumil and Wu were scaled to the values of this work.

that may explain the observed disagreement: wavelength shifts which were held constant even if the comparison between data at room temperature has shown that this is not the case; convolution to a very low resolution, and interpolation.

5. Conclusions

This paper, in combination with the PI paper, presents new absorption cross sections of SO_2 at high resolution and at temperature between 298 and 358 K covering a broad spectral region (24 000–44 000 cm^{-1}; 227–420 nm). A new extensive data set is therefore obtained which should be of particular interest for future planetary measurements. The complete data set comprising the absorption cross sections and their systematic and non-systematic errors at different temperatures is available in electronic format from the website of the Belgian Institute for Space Aeronomy: http://www.aeronomie.be/spectrolab/.

Literature data have been reviewed and compared to the present data at equivalent resolutions and coincident wavenumber scales. At room temperature, a very good agreement with most of the literature data is observed. It also shows that some of these data suffer from inaccurate wavelength calibration. The detailed comparison performed in this study gives an overview of what exists for this molecule and should be helpful for improving spectroscopic databases.

Literature data have been gathered in order to investigate the temperature dependence of SO_2 absorption cross sections. The decreasing trend of cross sections as a function of temperature is well established and the choice of a linear parametrization is a good approximation within each data set. However, it is far from perfect when combining the different data sets.

Acknowledgments

This project was supported by the National Fund for Scientific Research (FNRS FRFC convention no. 2.4542.08), by the Belgian Federal Science Policy Office (SSD program) and by the Communauté Française de Belgique (Actions de Recherche Concertées).

References

[1] Hermans C, Vandaele AC, Fally S. Fourier transform measurements of SO_2 absorption cross sections: I. Temperature dependence in the 24 000–29 000 cm−1 (345–420 nm) region. J Quant Spectrosc Radiat Transfer 2008;100:756–65.
[2] Möhler O, Arnold F. Gaseous sulfuric acid and sulfur dioxide measurements in the arctic troposphere and lower stratosphere: implications for hydroxyl radical abundances. Geophys Res Lett 1992;19:1763–6.
[3] Camy-Peyret C, Bergquist B, Galle B, Carleer M, Clerbaux C, Colin R, et al. Intercomparison of instruments for tropospheric measurements using differential optical absorption spectroscopy. J Atm Chem 1996;23:51–80.
[4] Vandaele AC, Tsouli A, Carleer M, Colin R. UV Fourier transform measurements of tropospheric O_3, NO_2, SO_2, benzene, and toluene. Environ Pollut 2002;116:193–201.
[5] Jaeschke W, Schmitt R, Georgii H-W. Preliminary results of stratospheric SO_2-measurements. Geophys Res Lett 1976;3:517–9.
[6] Krueger AJ. Sighting of el Chichón sulfur dioxide clouds with the Nimbus 7 total ozone mapping spectrometer. Science 1983;220:1377–9.
[7] Barker ES. Detection of SO_2 in the UV spectrum of Venus. Geophys Res Lett 1979;6:117–20.
[8] Bertaux J-L, Widemann T, Hauchecorne A, Moroz VI, Ekonomov AP. VEGA 1 and VEGA 2 entry probes: an investigation of local UV absorption (220–400 nm) in the atmosphere of Venus (SO_2, aerosols, cloud structure). J Geophys Res 1996;101:12709–46.

[9] Belayev D, Fedorova A, Korablev O, Vandaele AC, Mahieux A, Neefs E, et al. SO_2 detection in the Venus mesosphere with the SOIR spectrometer on board Venus Express. J Geophys Res 2008; doi:10.1029/2008JE003143.
[10] Esposito LW, Winick JR, Stewart AI. Sulfur dioxide in the Venus atmosphere: distribution and implications. Geophys Res Lett 1979;6:601–4.
[11] Bertaux JL, Belton MJS. Evidence of SO_2 on Io from UV observations. Nature 1979;282:813–5.
[12] Kim SJ, A'Hearn MF. Upper limits of SO and SO_2 in comets. Icarus 1991;90:79–95.
[13] Hamada Y, Merer AJ. Rotational structure at the long wavelength end of the 2900 Å system of SO_2. Can J Phys 1974;52:1443–57.
[14] Hillier IH, Saunders VR. A theoretical interpretation of the bonding, and the photoelectron and ultra-violet spectra of sulphur dioxide. Mol Phys 1971; 22:193–201.
[15] Brand JCD, Hardwick JL, Humphrey DR, Hamada Y, Merer AJ. Zeeman effects in the $A^1A_2 \leftarrow X^1A_1$ band system of sulfur dioxide. Can J Phys 1976; 54:186–96.
[16] Poulter KF, Rodgers M-J, Nash PJ, Thompson TJ, Perkin MP. Thermal transpiration correction in capacitance manometers. Vacuum 1983;33:311–6.
[17] Gerstenkorn S, Luc P. Absolute iodine (I_2) standards measured by means of Fourier transform spectroscopy. Rev Phys Appl 1979;14:791–4.
[18] Gerstenkorn S, Luc P. Atlas du spectre d'absorption de la molécule d'iode. France: Editions du CNRS; 1978.
[19] Edlén B. The refractive index of air. Metrologia 1966;2:71–80.
[20] Warneck P, Marmo FF, Sullivan JO. Ultraviolet absorption of SO_2: dissociation energies of SO_2 and SO. J Chem Phys 1964;40:1132–6.
[21] Vandaele AC, Simon PC, Guilmot JM, Carleer M, Colin R. SO_2 Absorption cross-section measurement in the UV using a Fourier transform spectrometer. J Geophys Res 1994;99:25599–605.
[22] Woods PT, Jolliffe BW, Marx BR. High-resolution spectroscopy of SO_2 using a frequency-doubled pulsed dye laser, with application to the remote sensing of atmospheric pollutants. Opt Commun 1980;33:281–91.
[23] Vattulainen J, Wallenius L, Stenberg J, Hernberg R, Linna V. Experimental determination of SO_2, C_2H_2, and O_2 UV absorption cross sections at elevated temperatures and pressures. Appl Spectrosc 1997;51:1311–5.
[24] Wu C-F, Yang BW, Chen F, Judge D, Caldwell JJ, Trafton LM. Measurements of high-, room-, and low-temperature photoabsorption cross sections of SO_2 in the 2080- to 2950-A region, with application to Io. Icarus 2000;145:289–96.
[25] Wu C-F, Judge D. SO_2 and CS_2 cross section data in the ultraviolet region. Geophys Res Lett 1981;8:769–71.
[26] Thompson Jr. RT, Hoell Jr. JM, Wade WR. Measurements of SO_2 absorption coefficients using a tunable dye laser. J Appl Phys 1975;46:3040–3.
[27] Rufus J, Stark G, Smith PL, Pickering JC, Thorne AP. High-resolution photoabsorption cross section measurements of SO_2, 2: 220 to 325 nm at 295 K. J Geophys Res 2003;108.
[28] Manatt SL, Lane AL. A compilation of the absorption cross-sections of SO_2 from 106 to 403 nm. J Quant Spectrosc Radiat Transfer 1993;50:267–76.
[29] McGee TJ, Burris Jr. J. SO_2 absorption cross sections in the near UV. J Quant Spectrosc Radiat Transfer 1987;37:165–82.
[30] Leroy B, Rigaud P, Jourdain JL, Le Bras G. Spectres d'absorption dans le proche ultraviolet de CS2 et SO_2 entre 200 et 300 K. Moon Planets 1983;29:177–83.
[31] Hearn CH, Joens JA. The near uv absorption spectrum of CS_2 and SO_2 at 300 K. J Quant Spectrosc Radiat Transfer 1991;45:69–75.
[32] Brassington DJ. Sulfur dioxide absorption cross-section measurements from 290 to 317 nm. Appl Opt 1981;20:3774–9.
[33] Bogumil K, Orphal J, Homann T, Voigt S, Spietz P, Fleischmann OC, et al. Measurements of molecular absorption spectra with the SCIAMACHY pre-flight model: instrument characterization and reference data for atmospheric remote-sensing in the 230–2380 nm region. J Photochem Photobiol A Chem 2003;157:167–84.
[34] Ahmed SM, Kumar V. Quantitative photoabsorption and fluorescence spectroscopy of SO_2 at 188–231 and 278.7–320 nm. J Quant Spectrosc Radiat Transfer 1992;47:359–73.
[35] Danielache SO, Eskebjerg C, Johnson M, Ueno Y, Yoshida N. High-precision spectroscopy of ^{32}S, ^{33}S, and ^{34}S sulfur dioxide: ultraviolet absorption cross sections and isotope effects. J Geophys Res 2008;113.